SCEC Award 20092

Technical Report

Update of operational GNSS products and development of integrated products for the CGM

Michael Floyd and Thomas Herring

Massachusetts Institute of Technology, Cambridge, MA, USA

Summary

We have implemented weekly operational generation of the CGM (continuous GNSS) time series from a combination of products from the Geodesy Advancing Geoscience and EarthScope (GAGE), Nevada Geodetic Laboratory (NGL), Jet Propulsion Laboratory (JPL), Scripps Orbital and Permanent Array Center (SOPAC) and the U.S. Geological Survey (USGS) analysis centers (ACs). These have been made available to a community user for testing in SCEC projects and feedback accordingly.

We have hosted and participated in bi-weekly CGM (InSAR) virtual meetings to act as a bridge between the GNSS and InSAR Working Groups, as well as SCEC HQ and the community in general, and to guide the CGM Working Group as a whole.

We have also contributed to the CGM (InSAR) component by developing tropospheric delay correction estimates based on the principles currently used to calculate a priori values for GNSS processing. These are currently undergoing testing within the CGM (InSAR) Working Group to understand their utility and usefulness in reducing tropospheric noise in interferograms and interferometric time series.

1. Operational production of CGM (GNSS) time series

We are now operationally generating CGM (cGNSS) time series each week on Friday (day 5 of the GPS week), which include all data available from continuous GNSS ACs up to and including the previous Saturday (last day of the GPS week). This means that the CGM (cGNSS) product lags between 5 and 12 days behind the current day, depending on the day of the week. This day and lag are chosen to accommodate the production schedule of the ACs while retaining near-real time products, which may be of interested to some community users.

Figure 1 shows, for site P617, the original time series from the ACs (left column) before restoration of any estimated and removed scale factor, and reweighting of the daily sigmas by a constant value for all times and all components at all sites from each AC (right column); the combined CGM (cGNSS) product is also shown (red time series in right column). The reweighting factor for the sigmas is chosen to reproduce a normalized root-mean-square residual to a fit of the time series of approximately 1. The values used for each analysis center and misfit statistics for the original and reweighted products are provided in Table 1.

We have communicated specifically with the SOPAC and USGS analysis centers, requesting them to provide raw products that are compatible with other analysis centers and therefore appropriate for inclusion in our CGM (cGNSS) combination, as well as to verify

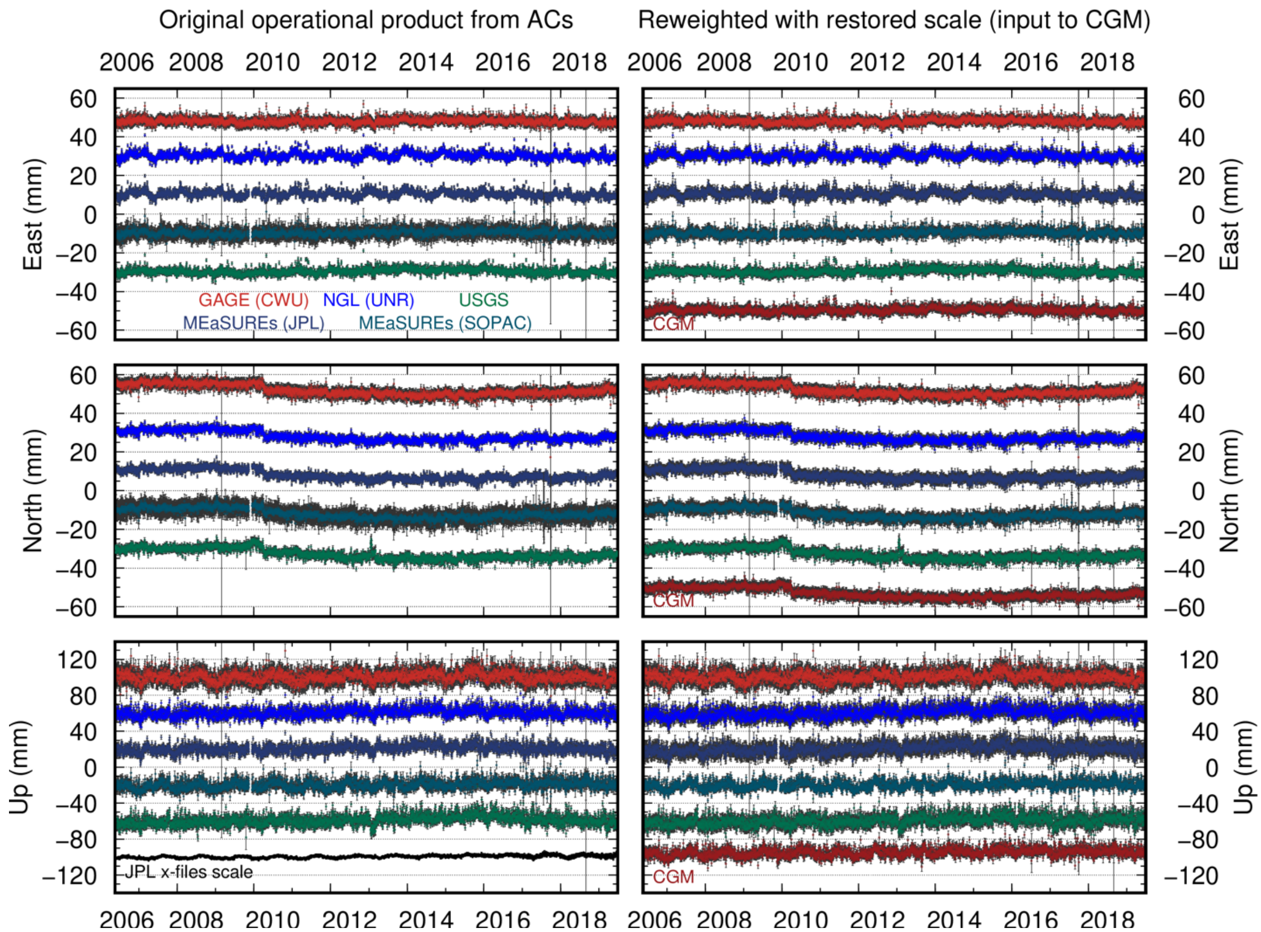

Figure 1: Pre-Ridgecrest raw, adjusted and combined CGM time series for site NOTA site P617, which acts as the reference pixel for tracks 64 and 71 currently being finalized for the CGM (InSAR) time series. Left column: Original source analysis center products before scaling of uncertainties (see Table 1) and restoration of scale (Gipsy-processed products from NGL (UNR), MEaSUREs (JPL) and USGS only) for input to the CGM combination; the up component also shows the height variation that is effectively removed when a scale adjustment is estimated and applied. Right columns: Reweighted and scaled products and the final CGM combination. The discontinuity seen in the north component of all time series is due to the 2010-04-04 El Mayor-Cucapah earthquake.

missing information as necessary, such as which set of JPL-provided scaling parameters were used during processing with the Gipsy software in the case of the USGS. We now have all the information necessary to produce a consistent product.

As soon as survey time series processing and generated by Z.-K. Shen (UCLA) are provided to us in a compatible file format, we will also include these episodic GNSS time series in our combination in a consistent reference frame. These will soon be uploaded to Zenodo (https://zenodo.org/), with a unique digital object identifier (DOI) per weekly submission, via their API, with which we are currently experimenting for automated uploads. Our products to date have been "beta-tested" over the last few months since the 2020 SCEC Annual Meeting by Lauren Ward and Bridget Smith-Konter at the University of Hawaii as part of their SCEC work.

Table 1: Median NRMS statistics based on the fit of IGb14 core sites to the IGb14 reference frame and on a linear fit to the time series, before and after application of a reweighting factor to the time series uncertainties (sigma factor > 1 means downweighting relative to the standard deviations in the original time series). The NRMS (U) value in square brackets for the NGL and JPL time series is calculated before the restoration of estimated scale.

Analysis Center	Reference frame (before)	Time series (before)	Reference frame (after)	Time series (after)	Sigma factor
GAGE (CWU)	1.33 (N) 1.80 (E) 1.26 (U)	0.74 (N) 0.83 (E) 0.82 (U)	1.33 (N) 1.80 (E) 1.26 (U)	0.74 (N) 0.83 (E) 0.82 (U)	1.0
NGL (UNR)	1.59 (N) 2.16 (E) 1.97 [1.89] (U)	1.96 (N) 2.33 (E) 1.89 [1.95] (U)	0.63 (N) 0.87 (E) 0.80 (U)	0.88 (N) 1.02 (E) 0.76 (U)	2.5
JPL	2.08 (N) 2.53 (E) 3.03 [3.09] (U)	2.29 (N) 2.31 (E) 2.41 [2.42] (U)	0.74 (N) 0.91 (E) 1.09 (U)	0.95 (N) 0.93 (E) 0.86 (U)	2.8
SOPAC	0.46 (N) 0.48 (E) 1.51 (U)	0.74 (N) 0.35 (E) 1.03 (U)	0.65 (N) 0.69 (E) 2.15 (U)	1.04 (N) 0.50 (E) 1.47 (U)	0.7
USGS	1.62 (N) 1.47 (E) 2.03 [2.21] (U)	1.17 (N) 1.01 (E) 1.62 [1.68] (U)	1.15 (N) 1.06 (E) 1.27 (U)	0.91 (N) 0.79 (E) 1.06 (U)	1.6

2.a. CGM (InSAR) Working Group activities

Led by Katia Tymofyeyeva (JPL), we have assisted in hosting and guiding the CGM (InSAR) Working Group in their research for contributing to a combined geodetic product for the CGM. We are now ready to offer at least one track (descending track 71) for testing via the SCEC CGM web viewer, which we anticipate will be offered to a select group of interested community users within the next few weeks. Our role in these meetings has mostly been to speak on behalf of the CGM (GNSS) Working Group and SCEC's goals for the CGM in general, to ensure that the InSAR Working Group remains focused on the mission of generating community products.

2.b. Estimation of tropospheric delay from GNSS principles for InSAR

The ultimate integration of GNSS and InSAR time series and velocity products relies to a great extent on the fundamental compatibility between models applied to both time series consistently. For example, GNSS processing regularly models solid Earth and ocean tide loading to account for the large displacements induced by these phenomena that are not necessarily of interest for tectonic geodesy. InSAR processing software such as GMTSAR are now able to incorporate tidal displacements. However, another significant source of error is the effect of phase propagation through the atmosphere, including both the troposphere and ionosphere.

We have applied the same methods used to calculate a priori tropospheric delay estimates for GNSS processing, to which an adjustment is ultimately estimated during the data processing, and our estimates are now undergoing testing with the CGM (InSAR) group's processing to ascertain if our approach reduces tropospheric noise for InSAR time series. There are three parts to any GNSS-processed tropospheric delay estimate: the a priori zenith hydrostatic delay, which is usually assumed sufficiently accurate and held fixed; the a priori zenith "wet" delay; and the adjustment to the a priori zenith wet delay estimated during data processing, which has an associated uncertainty that is generally applicable to the sum of the delays, the zenith total delay. One may reasonably relate the sum of the first two quantities to the "stratified" atmospheric term, *S*, in the currently common GACOS formulation (Yu et al., 2017) for InSAR tropospheric delay estimation.

Instead of assuming a delay from the stratified troposphere taking the form $L_0 e^{-\beta h}$, where L_0 and β are estimated as constants, although we know they must be spatially variable, we have instead calculated this term using the results of a publicly available service which performs ray-tracing through the numerical weather model of the European Centre for Medium-Range Weather Forecasting (ECMWF) to obtain estimates of the zenith hydrostatic and wet delays. The latest iteration of this product is the Vienna Mapping Function 3 (VMF3; Landskron and Böhm, 2018). Using equations that approximate the change of pressure, temperature, water vapor pressure and temperature weighted by water vapor pressure as a function of height, and therefore the change in zenith hydrostatic and wet delays (Berg, 1948; Hopfield, 1969; Askne and Nordius, 1987), we calculate the stratified tropospheric delay across variable topography from the VMF3 values, which are defined on a 1°×1° grid at heights associated with each grid point.

The difference between these a priori zenith delay estimates, assuming a stratified

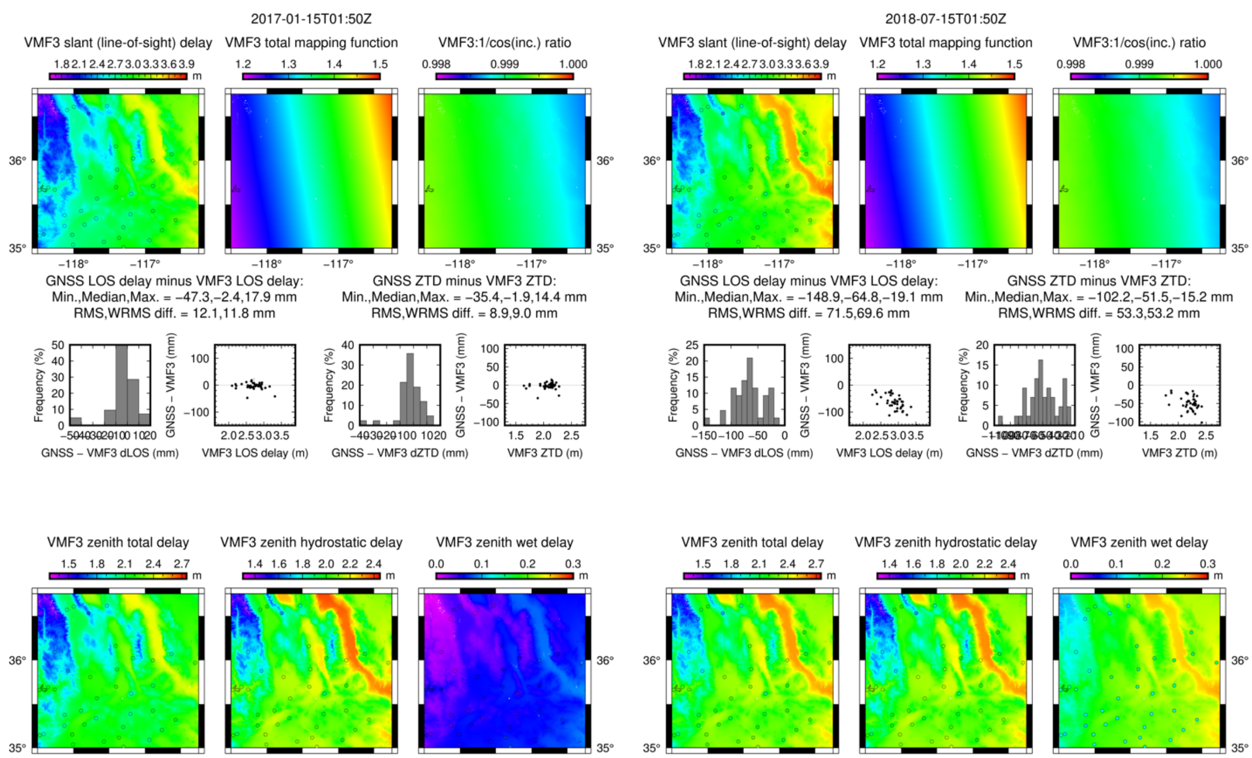

Figure 2: "Best" (left) and "worst" (right) examples for track 64, showing the range of fits of our estimated delay through a stratified troposphere from the VMF compared to the GNSS estimates available over the region, before the addition of a turbulent term estimated from the GNSS residual delay, as described in the text. Most acquisition times have a VMF-only (no-GNSS) RMS misfit of 15-30 mm.

troposphere, and any available GNSS zenith total delay estimates may be considered to correspond to the "turbulent" tropospheric term in Yu et al.'s (2017) GACOS formulation. The residual delay may be fit to a continuous surface at the resolution of the InSAR data by bilinear interpolation, as we have done here, or by the approach described by Yu et al. (2017).

As part of this calculation, the mapping function (multiplication factor between zenith delay and slant (line-of-sight) delay) is also estimated for the variable incidence angle of the SAR signal across the region. Figure 2 shows the calculated hydrostatic, "wet" and total zenith tropospheric delays (bottom row) in addition to the slant (line-of-sight) delay using the total mapping function show in the top-center and its ratio to the commonly used trigonometric mapping function 1/cos(incidence angle).

References

Askne, J., and Nordius, H. (1987), Estimation of tropospheric delay for microwaves from surface weather data, *Radio Sci.*, *22*, 379–386, doi:10.1029/RS022i003p00379.

Berg, H. (1948), Allgemeine Meteorologie, Dümmler, Bonn.

Hopfield, H. S. (1969), Two-quartic tropospheric refractivity profile for correcting satellite data, *J. Geophys. Res.*, 74, 4487–4499, doi:10.1029/JC074i018p04487.

Landskron, D., and Böhm, J. (2018), VMF3/GPT3: refined discrete and empirical troposphere mapping functions, *J. Geod.*, *92*, 349–360, doi:10.1007/s00190-017-1066-2.

Yu, C., Penna, N. T., and Li, Z. (2017), Generation of real-time mode high-resolution water vapor fields from GPS observations, *J. Geophys. Res. Atmos.*, *122*, 2008– 2025, doi:10.1002/2016JD025753.